

# Regioselectivity of the Oxidative C–S Bond Formation in Ergothioneine and Ovothiol Biosyntheses

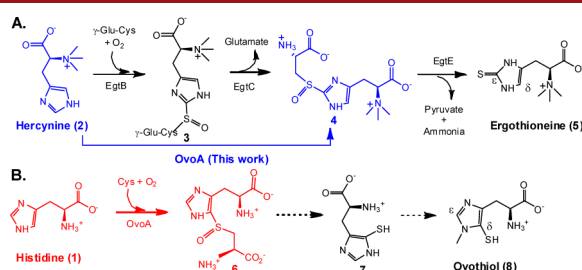
Heng Song, Maureen Leninger, Norman Lee, and Pinghua Liu\*

Department of Chemistry, Boston University, Boston, Massachusetts 02215, United States

pinghua@bu.edu

Received August 9, 2013

## ABSTRACT



Ergothioneine (5) and ovothiol (8) are two novel thiol-containing natural products. Their C–S bonds are formed by oxidative coupling reactions catalyzed by EgtB and OvoA enzymes, respectively. In this work, it was discovered that in addition to catalyzing the oxidative coupling between histidine and cysteine (1  $\rightarrow$  6 conversion), OvoA can also catalyze a direct oxidative coupling between hercynine (2) and cysteine (2  $\rightarrow$  4 conversion), which can shorten the ergothioneine biosynthetic pathway by two steps.

Sulfur is an important functional group in both primary and secondary metabolites.<sup>1</sup> Biological sulfur transfer reactions can make use of either an ionic or radical type of reaction mechanism. For example, the thioether formation in lantibiotic biosynthesis is an ionic type of reaction that is accomplished by having thiolates as the direct nucleophiles.<sup>2</sup> Radical type C–S bond formation reactions are also well-documented.<sup>1a,3</sup> Some of the

examples are the incorporation of the thiol functional groups into biotin,<sup>4</sup> lipoate,<sup>3a</sup> thiamine pyrophosphate,<sup>5</sup> and molybdopterin cofactor,<sup>6</sup> cofactor biogenesis in galactose oxidase,<sup>7</sup> tRNA nucleotide thiolmethylation,<sup>8</sup> and thiazolidine ring formation catalyzed by isopenicillin N synthase.<sup>9</sup> For sulfur transfer reactions, two types of activated sulfur species have also been discovered,<sup>10</sup> which are persulfides R–S–SH and thiocarboxylates R–CO–SH.

Ergothioneine (5) and ovothiol (8) are two thiol-imidazole-containing natural products. Humans obtain ergothioneine from their diet and specifically enrich it in some tissues (e.g., liver, kidney, central nervous system, and red blood cells) by using an ergothioneine-specific transporter.<sup>11</sup> Ergothioneine's beneficial effects to human health are due to its unusual redox properties, which

(1) (a) Fontecave, M.; Ollagnier-de-Choudens, S.; Mulliez, E. *Chem. Rev.* **2003**, *103*, 2149. (b) Kessler, D. *FEMS Microbiol. Rev.* **2006**, *30*, 825. (c) Hand, C. E.; Honek, J. F. *J. Nat. Prod.* **2005**, *68*, 293. (d) Fahey, R. C. *Annu. Rev. Microbiol.* **2001**, *55*, 333. (e) Lin, C.-I.; McCarty, R. M.; Liu, H.-w. *Chem. Soc. Rev.* **2013**, *42*, 4377. (f) Parry, R. J. In *Comprehensive Natural Products Chemistry I*; Barton, D., ; Nakanishi, K., Meth-Cohn, O., Ed.; Pergamon: Oxford, U.K., 1999, Vol. 1, p 825. (g) Wang, L.; Chen, S.; Xu, T.; Taghizadeh, K.; Wishnok, J.; Zhou, X.; You, D.; Deng, Z.; Dedon, P. *Nat. Chem. Biol.* **2007**, *3*, 709. (h) Scharf, D. H.; Remme, N.; Habel, A.; Chankhamjon, P.; Scherlach, K.; Heinekamp, T.; Hortschansky, p.; Brakhage, A. A.; Hertweck, C. *J. Am. Chem. Soc.* **2011**, *133*, 12322. (i) Wang, Q.; Song, F.; Xiao, X.; Huang, P.; Monte, A.; Abdel-Mageed, W. M.; Wang, J.; Guo, H.; He, W.; Xie, F.; Dai, H.; Liu, M.; Chen, C.; Xu, H.; Liu, M.; Piggott, A. M.; Liu, X.; Capon, R. J.; Zhang, L. *Angew. Chem., Int. Ed.* **2013**, *52*, 1231.

(2) Willey, J. M.; van der Donk, W. A. *Annu. Rev. Microbiol.* **2007**, *61*, 477.

(3) (a) Booker, S. J.; Cicchillo, R. M.; Grove, T. L. *Curr. Opin. Chem. Biol.* **2007**, *11*, 543. (b) Parry, R. J. *Tetrahedron* **1983**, *39*, 1215.

(4) Fugate, C. J.; Jarrett, J. T. *Biochim. Biophys. Acta, Proteomics* **2012**, *1824*, 1213.

(5) Jurgenson, C. T.; Begley, T. P.; Ealick, S. E. *Annu. Rev. Biochem.* **2009**, *78*, 569.

(6) (a) Schwarz, G.; Mendel, R. R. *Annu. Rev. Plant Biol.* **2006**, *57*, 623. (b) Leimkuhler, S.; Klipp, W. *FEMS Microbiol. Lett.* **1999**, *174*, 239.

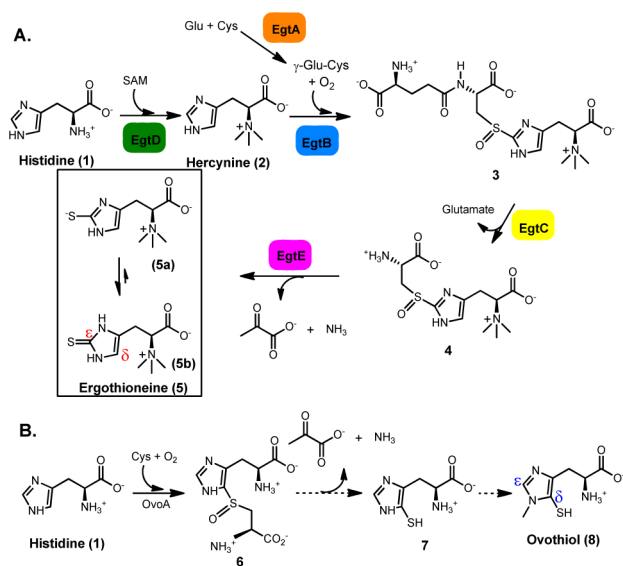
(7) Whittaker, J. W. *Arch. Biochem. Biophys.* **2005**, *433*, 227.

(8) Kessler, D. *FEMS Microbiol. Rev.* **2006**, *30*, 825.

(9) Baldwin, J. E.; Bradley, M. *Chem. Rev.* **1990**, *90*, 1079.

(10) (a) Mueller, E. G. *Nat. Chem. Biol.* **2006**, *2*, 185. (b) Johnson, D. C.; Dean, D. R.; Smith, A. D.; Johnson, M. K. *Annu. Rev. Biochem.* **2005**, *247*.

**Scheme 1. Proposed Ergothioneine and Ovothiol Biosynthetic Pathways**



favor predominantly the thione form (5b, Scheme 1A) and make ergothioneine much more stable than most other natural thiols.<sup>1c,d,11g</sup> Ergothioneine was isolated from ergot by Tanret in 1909,<sup>12</sup> and its biosynthetic gene cluster was reported by Seebeck in 2010 (Scheme 1A).<sup>13</sup> Ergothioneine biosynthesis starts from histidine methylation to trimethylated histidine (hercynine, 2), which is then oxidatively coupled with  $\gamma$ -glutamylcysteine ( $\gamma$ -Glu-Cys) to 3. After glutamate is removed by hydrolysis, a PLP-containing enzyme (EgtE) catalyzes the 4  $\rightarrow$  5 conversion. Ovothiol is another thiol–histidine enriched in the eggs of many marine species. Ovothiol is proposed to be involved in  $H_2O_2$  scavenging and facilitation of the fertilization process.<sup>14</sup> For ovothiol biosynthesis (Scheme 1B), the only known enzyme is OvoA, which catalyzes the oxidative coupling between Cys and His (1  $\rightarrow$  6 conversion).<sup>15</sup> In comparison to ergothioneine, the C–S bond in ovothiol is at the  $\delta$  instead of the  $\epsilon$  position.

Both EgtB and OvoA are mononuclear nonheme iron enzymes catalyzing four-electron oxidation processes (Scheme 1). However, EgtB and OvoA distinguish themselves from each other by their substrate preferences and product C–S bond regioselectivity (Scheme 1). Ergothioneine’s thiol group is located at its imidazole  $\epsilon$  carbon,

while ovothiol’s thiol group is at its imidazole  $\delta$  carbon. In addition, EgtB and OvoA use different substrates. EgtB catalyzes the oxidative coupling between hercynine (2) and  $\gamma$ -Glu-Cys, while OvoA preferentially oxidatively couples His and Cys. In this report, a key factor governing OvoA-catalyzed regioselectivity was discovered. By systematic modulation of the histidine methylation state, the OvoA catalysis changes from an OvoA type of chemistry (1  $\rightarrow$  6 conversion) to an EgtB type of chemistry (2  $\rightarrow$  4 conversion). Such a discovery can shorten the ergothioneine biosynthetic pathway by two steps.

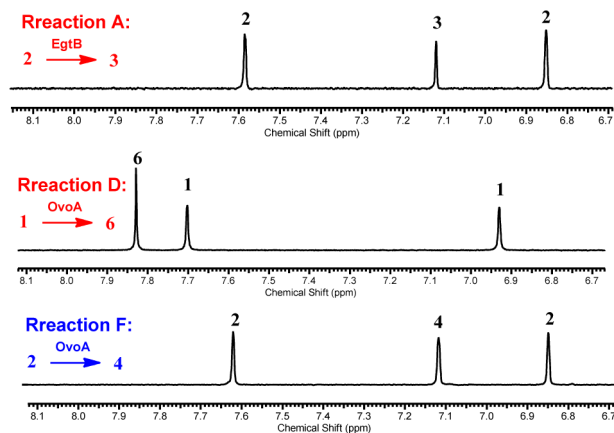


**Figure 1.**  $^1H$  NMR assay (chemical shifts of imidazole ring H atoms). Reaction A: native EgtB reaction in ergothioneine biosynthesis. The chemical shift assignments are as follows: 3, the imidazole H atom of compound 3 (7.12 ppm); 2, the hercynine imidazole H atoms (6.85, 7.58 ppm). Reaction D: native OvoA reaction in ovothiol biosynthesis. The chemical shift assignments are as follows: 6, the imidazole H atom of compound 6 (7.83 ppm); 1, the imidazole H atoms of His (6.93, 7.70 ppm). Reaction F: a new OvoA reaction (oxidative coupling between hercynine and Cys). In this case, the oxidative coupling product is compound 4, which has the EgtB type of regioselectivity. Reaction list is shown in Scheme 2.

EgtB and OvoA were overexpressed in *E. coli* and purified anaerobically using Strep-tavidin affinity chromatography (Figure 1S, Supporting Information). The purified proteins have close to a stoichiometric amount of iron. To examine EgtB and OvoA substrate specificity, a  $^1H$  NMR assay was utilized (Figure 1). In the  $^1H$  NMR spectrum, the chemical shifts of the EgtB product (3) imidazole H atom, OvoA product (6) imidazole H atom, and the substrate (histidine) are well-separated from the rest of the reaction mixture (Figure 1). Thus, the reaction mixture can be analyzed routinely without the need for product separation (Figure 1). The signals with chemical shifts of 6.93 and 7.70 ppm are assigned to the histidine imidazole H atoms. The signal at 7.83 ppm is from the imidazole H atom of ovothiol biosynthetic intermediate 6 (reaction D, Figure 1), while for the oxidative product 3 in ergothioneine biosynthesis, its imidazole H atom has a chemical shift of 7.12 ppm (reaction A, Figure 1).

Using the  $^1H$  NMR assay, we systematically examined EgtB and OvoA substrate binding pocket flexibility

(11) (a) Grundemann, D.; Harlfinger, S.; Golz, S.; Geerts, A.; Lazar, A.; Berkels, R.; Jung, N.; Rubbert, A.; Schomig, E. *Proc. Natl. Acad. Sci. U.S.A.* **2005**, *102*, 5256. (b) Melville, D. B.; Eich, S. *J. Biol. Chem.* **1956**, *218*, 647. (c) Fahey, R. C.; Newton, G. L.; Dorian, R.; Kosower, E. M. *Anal. Biochem.* **1981**, *111*, 357. (d) Genghof, D. S.; Inamine, E.; Kovalenko, V.; Melville, D. B. *J. Biol. Chem.* **1956**, *223*, 9. (e) Briggs, I. *J. Neurochem.* **1972**, *19*, 27. (f) Epand, R. M.; Epand, R. F.; Wong, S. C. *J. Clin. Chem. Clin. Biochem.* **1988**, *26*, 623. (g) Hartman, P. E. *Methods Enzymol.* **1990**, *186*, 310.

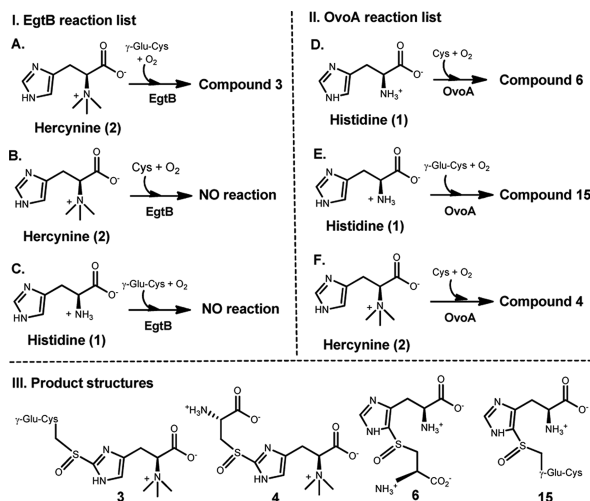
(12) Tanret, C. *Compt. rend.* **1909**, *149*, 222.

(13) Seebeck, F. P. *J. Am. Chem. Soc.* **2010**, *132*, 6632.

(14) Turner, E.; Klevit, R.; Hager, L. J.; Shapiro, B. M. *Biochemistry.* **1987**, *26*, 4028.

(15) Braunshausen, A.; Seebeck, F. P. *J. Am. Chem. Soc.* **2011**, *133*, 1757.

## Scheme 2. Examining EgtB and OvoA Substrate Specificities



(Scheme 2). EgtB does not accept OvoA's substrates as its alternative substrates (reactions B and C, Scheme 2). Interestingly, OvoA has much more flexibility in substrate specificity. OvoA can accept  $\gamma$ -Glu-Cys as a substrate and oxidatively couples it with His to form compound **15** (reaction E, Scheme 2). OvoA also can accept hercynine (**2**) as a substrate (reaction F, Scheme 2). More interestingly, the  $^1\text{H}$  NMR spectrum of this reaction gives a new signal at 7.12 ppm (reaction F, Figure 1). In comparison with the  $^1\text{H}$  NMR spectra of the native EgtB reaction (reaction A, Figure 1) and native OvoA reaction (reaction D, Figure 1), the 7.12 ppm signal highly suggests that compound **4** is the product from the OvoA-catalyzed oxidative coupling between Cys and hercynine (Scheme 2, reaction F in Figure 1 and Figure 11S (Supporting Information)). The formation of **4** implies a change in OvoA regioselectivity from the OvoA type (reaction D, Figure 1) to the EgtB type (reaction F, Figure 1) upon the change of histidine to hercynine.

To provide further evidence to support the structural assignment of compound **4**, it was isolated and characterized by mass spectrometry and several NMR spectra ( $^1\text{H}$  NMR,  $^{13}\text{C}$  NMR, and 2D-NMR including COSY, HMBC, and HMQC, Figure 2 and Figures 12S–17S (Supporting Information)).  $^1\text{H}$ – $^{13}\text{C}$  correlations between H-5 and C-4, C-6 in HMBC characterization support the structural assignment of compound **4** (Figure 2). Additional cross-peaks (between H-3' and C-6 and between H-3 and C-4, C-5, Figure 2) are also consistent with the compound **4** structure. HMQC spectrum suggests that the only proton in the compound **4** imidazole ring ( $\delta$  7.45 ppm) is at the histidine  $\delta$  carbon (122 ppm, Figure 16S (Supporting Information)), which provides additional evidence for an OvoA-catalyzed direct **2**  $\rightarrow$  **4** conversion. In the spectra of Figure 2 and Figure 16S, in order to resolve the resonances in the 3.0–4.5 ppm region, the sample was acidified. As a result, the imidazole ring hydrogen chemical shift (Figure 2) is now at 7.45 ppm instead of 7.12 ppm in Figure 1.

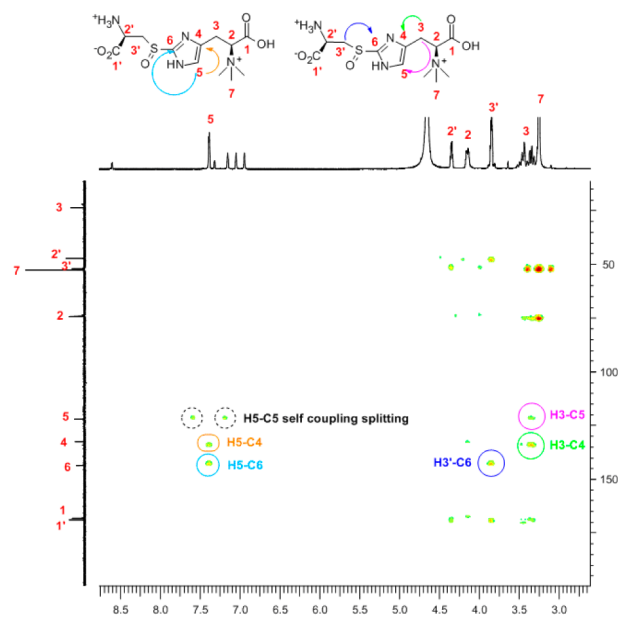
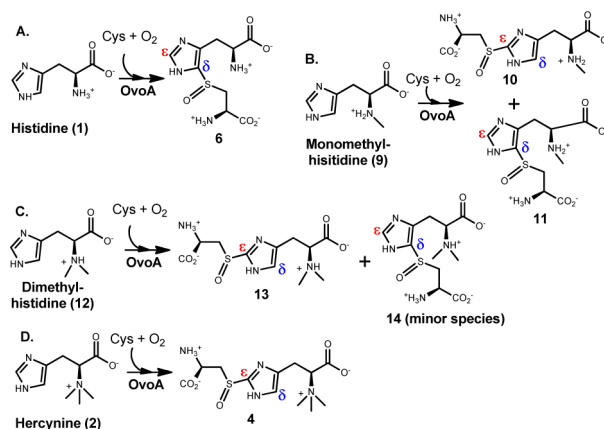


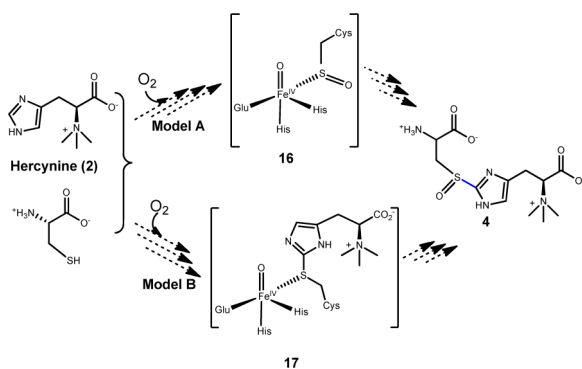
**Figure 2.** HMBC-NMR analysis of compound **4**. H-5 shows  $^1\text{H}$ – $^{13}\text{C}$  correlations between C-4 (orange circle) and C-6 (cyan arrow). Additional cross-peaks between H-3' and C-6 (blue circle), H-3 and C-4 (green circle), and H-3 and C-5 (pink circle) are also shown.

## Scheme 3. New OvoA Chemistries



Upon the change of histidine to hercynine, OvoA changes its oxidative C–S bond formation regioselectivity. This result highly suggests that the OvoA binding pocket for the histidine amino group plays a key role in determining the imidazole ring binding orientation, which in turn determines the oxidative C–S bond formation regioselectivity. To test this hypothesis, mono- and dimethylhistidine were synthesized. Indeed, OvoA can also make use of them as alternative substrates. Interestingly, when monomethylhistidine (**9**) and cysteine are used as the substrates, OvoA produces two oxidative coupling products, compound **10** and compound **11**, in a ratio of 2:3 (Scheme 3

**Scheme 4.** Two OvoA Mechanistic Routes



and Figure 19S (Supporting Information)). In the case of dimethylhistidine (**12**), compound **13** is the dominant product and compound **14** is barely detectable in our  $^1\text{H}$  NMR assay (Scheme 3 and Figure 20S (Supporting Information)). Results from these studies indicate that the OvoA substrate binding pocket for the histidine amino group plays a key role in orienting substrates in the enzyme active site, which in turn determines the oxidative C–S bond formation regioselectivity (Scheme 3).

In air-saturated HEPES buffer ( $\sim 250\ \mu\text{M}$  of oxygen), these new OvoA reactions were characterized kinetically by monitoring the oxygen consumption rate using the NeoFoxy oxygen electrode. (A) When histidine and cysteine are the substrates, the kinetic parameters are  $k_{\text{obs}} = 572 \pm 20\ \text{min}^{-1}$  and  $K_{\text{m}} = 420 \pm 31\ \mu\text{M}$  for His and  $K_{\text{m}} = 300 \pm 34\ \mu\text{M}$  for Cys. (B) When Cys and monomethylhistidine (**9**) are the substrates, the kinetic parameters are  $k_{\text{obs}} = 527 \pm 10\ \text{min}^{-1}$  and  $K_{\text{m}}$  of  $466 \pm 32\ \mu\text{M}$  for monomethylhistidine and  $K_{\text{m}} = 0.99 \pm 0.05\ \text{mM}$  for Cys. (C) When Cys and dimethylhistidine (**12**) are the substrates, the kinetic parameters are  $k_{\text{obs}} = 367 \pm 8\ \text{min}^{-1}$  and  $K_{\text{m}} = 466 \pm 38\ \mu\text{M}$  for hercynine and  $K_{\text{m}} = 1.61 \pm 0.12\ \text{mM}$  for Cys. (D) When Cys and hercynine (**2**) are the substrates, the kinetic parameters are  $k_{\text{obs}} = 270 \pm 5\ \text{min}^{-1}$  and  $K_{\text{m}} = 395 \pm 30\ \mu\text{M}$  for hercynine and  $K_{\text{m}} = 3.19 \pm 0.41\ \text{mM}$  for Cys.

In summary, our studies here revealed that OvoA has a very relaxed substrate binding pocket and can accept EgtB substrates as alternatives. Moreover, by modulation of the histidine amino group methylation state, the

regioselectivity of OvoA catalysis changes from the OvoA type to the EgtB type (Scheme 3). Due to many of ergothioneine's beneficial roles in human health,<sup>1c,16</sup> there is a longstanding interest in developing more efficient methods for its production.<sup>17</sup> The discovery of this unique OvoA chemistry (a direct **2**  $\rightarrow$  **4** conversion) suggests that such a chemistry may be further explored for future ergothioneine production through metabolic engineering. This transformation not only shortens the ergothioneine biosynthetic pathway by two steps (elimination of EgtA and EgtC steps; see Scheme 1) but also eliminates the competition between ergothioneine and glutathione biosyntheses because  $\gamma$ -Glu-Cys is a substrate in both the EgtB reaction and glutathione biosynthesis.

Several mechanistic models have been proposed for oxidative C–S bond formation in EgtB and OvoA catalysis since their discovery.<sup>15,18</sup> The oxidative C–S bond formation in OvoA and EgtB seems to be distinct from currently known biological C–S bond formation mechanisms.<sup>1a,c,d,8</sup> Thus far, mechanistic evidence is not yet available for differentiating among the proposed mechanistic options in the literature. Both EgtB and OvoA catalyze four-electron oxidation processes, and two different functional groups are constructed in these reactions (sulfoxide and C–S bond, Scheme 4). Thus, the first mechanistic issue to be addressed in OvoA and EgtB catalysis is whether the sulfenic acid formation (model A) or the C–S bond formation (model B) is the first step. This mechanistic question is currently under investigation in our laboratory.

**Acknowledgment.** This work was partially supported by an NSF award (CHE-1309148) and an NIH award (GM093903) to P.L. We thank the NSF (CHE0619339, CHE 0443618) for the 500 MHz NMR and high-resolution mass spectrometers used in this work. We also thank the NSF (DBI0959666) for the Perkin-Elmer Elan 6100 DRC instrument and Drs. Robyn Hannigan, Alan Christian, and Bryanna J. Broadaway (University of Massachusetts Boston) for Fe analyses. We thank Prof. John Snyder for help in NMR analysis.

**Supporting Information Available.** Text and figures giving experimental procedures, characterization data, and  $^1\text{H}$  and  $^{13}\text{C}$  NMR spectra of the synthesized compounds **2**, **4**, and **6**. This material is available free of charge via the Internet at <http://pubs.acs.org>.

(16) (a) Weaver, K. H.; Rabenstein, D. L. *J. Org. Chem.* **1995**, *60*, 1904. (b) Scott, E. M.; Duncan, I. W.; Ekstrand, V. *J. Biol. Chem.* **1963**, *238*, 3928.

(17) (a) Xu, J.; Yadan, J. C. *J. Org. Chem.* **1995**, *60*, 6296. (b) Erdelmeier, I.; Daunay, S.; Lebel, R.; Faescour, L.; Yadan, J. C. *Green Chem.* **2012**, *14*, 2256.

(18) (a) Bushnell, E. A.; Fortowshy, G. B.; Gauld, J. W. *Inorg. Chem.* **2012**, *51*, 13351. (b) Mashabela, G. T.; Seebeck, F. P. *Chem. Commun.* **2013**, *49*, 7714.

The authors declare no competing financial interest.